Design, fabrication and characterization of LVOF-based IR microspectrometers

N.P. Ayerden[*a], M. Ghaderi[a], M. F. Silva[d], A. Emadi[b], P. Enoksson[c], J.H. Correia[d], G. de Graaf[a], and R.F. Wolffenbuttel[a]

[a]Faculty of EEMCS, Delft University of Technology, Mekelweg 4, 2628 CD, Delft, Netherlands; [b]Maxim Integrated, San Francisco Bay Area, Electrical/Electronic Manufacturing; [c]Micro and Nanosystems, MC2, Chalmers University of Technology, SE-412 96, Gothenburg, Sweden; [d]Dept. of Industrial Electronics, University of Minho, Campus Azurem, 4800-058 Guimarães, Portugal

ABSTRACT

This paper presents the design, fabrication and characterization of a linear variable optical filter (LVOF) that operates in the infrared (IR) spectral range. An LVOF-based microspectrometer is a tapered-cavity Fabry-Perot optical filter placed on top of a linear array of detectors. The filter transforms the optical spectrum into a lateral intensity profile, which is recorded by the detectors. The IR LVOF has been fabricated in an IC-compatible process flow using a resist reflow and is followed by the transfer etching of this resist pattern into the optical resonator layer. This technique provides the possibility to fabricate a small, robust and high-resolution micro-spectrometer in the IR spectral range directly on a detector chip. In these designs, the LVOF uses thin-film layers of sputtered Si and SiO_2 as the high and low refractive index materials respectively. By tuning the deposition conditions and analyzing the optical properties with a commercial ellipsometer, the refractive index for Si and SiO_2 thin-films was measured and optimized for the intended spectral range. Two LVOF microspectrometers, one operating in the 1.8-2.8 μm, and the other in the 3.0-4.5 μm wavelength range, have been designed and fabricated on a silicon wafer. The filters consist of a Fabry-Perot structure combined with a band-pass filter to block the out-of-band transmission. Finally, the filters were fully characterized with an FTIR spectrometer and the transmission curve widening was investigated. The measured transmittance curves were in agreement with theory. The characterization shows a spectral resolution of 35-60 nm for the short wavelength range LVOF and 70 nm for the long wavelength range LVOF, which can be further improved using signal processing algorithms.

Keywords: Spectroscopy, Fabry-Perot, Bragg reflector, LVOF, infrared, gas sensor, natural gas, hydrocarbons

1. INTRODUCTION

Natural gas has been a major source of energy, especially in the Netherlands due to the availability of local resources in Groningen. However, the depletion of natural gas resources will force a transition from domestic Groningen gas (G-gas) towards 'new' gas in the coming years (Figure 1). The 'new' gas will be a mixture of G-gas and high-calorific-value gas (H-gas) imported from other countries such as Russia and Norway, liquefied natural gas (LNG), and biogas [1]. Typical composition of G-gas, H-gas and LNG are summarized in Table 1. In addition to these components, biogas includes H_2. With the addition of all these gases, the composition of the gas that is supplied to the user will change from the very stable G-gas composition to the unknown 'new' gas. Therefore, the adaptation to the new composition will require composition measurement at many local distribution points, which requires gas sensors that are easily installable, small, compact, robust and low-cost to ensure safe and clean combustion.

The transmission spectra of the main components in natural gas were adapted from NIST database [2]. The absorption coefficients of individual components were extracted using typical concentrations of G-gas at room temperature with 1 bar total pressure. Hydrocarbons have significant absorption peaks in 3-3.7 μm wavelength range as shown in Figure 2. In addition, methane (CH_4) has less significant peaks in 2.5-3 μm range. Although the hydrocarbons have strong absorption in 3-3.7 μm wavelength range, especially higher hydrocarbons have similar spectra. Thus, differentiating these gases requires a spectroscopic technique with high resolution as well as post data processing. Carbon-dioxide has two peaks at 2.7 μm and 4.3 μm. Nitrogen and hydrogen have zero dipole moment; hence, they are defined as infrared

Micro-Optics 2014, edited by Hugo Thienpont, Jürgen Mohr, Hans Zappe, Hirochika Nakajima, Proc. of SPIE Vol. 9130, 91300T · © 2014 SPIE
CCC code: 0277-786X/14/$18 · doi: 10.1117/12.2052620

inactive. As a result, these two gases cannot be monitored by infrared spectroscopy techniques and another method should be used.

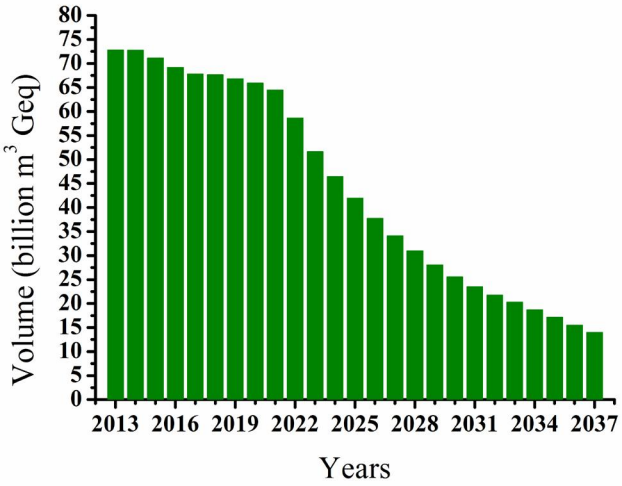

Figure 1: The expected natural gas production in the Netherlands [3]. (Geq stands for Groningen gas equivalent with a heating value of 35.17 MJ/Nm^3.)

A wide range of techniques for gas sensing is available. The simplest sensor for gas analysis is a pellistor. A pellistor is a non-selective and low cost micro-calorimetric sensor that measures the temperature change resulting from gas oxidation. On the other end of the range lies the gas chromatograph, which is a high resolution and high cost equipment suitable for lab use. Optical absorption spectroscopy is a promising compromise between cost and performance in gas sensing. The technique enables *in situ* measurements without physical contact with the sample. Moreover, the self-referencing property makes optical absorption more reliable compared to other gas sensing techniques [4].

Table 1: Typical composition of G-gas, H-gas, and LNG.

	CH_4 [mol %]	C_2H_6 [mol %]	C_3H_8 [mol %]	C_4H_{10} [mol %]	CO_2 [mol %]	N_2 [mol %]
G-Gas	82.3	3.07	0.47	0.09	1.1	12.7
H-Gas	89	5.3	1.3	0.3	1.2	2.3
LNG	90	6.25	1	2.1	1	1.1

In optical absorption spectroscopy light is passed through a sample and the ratio of absorbed to incident radiation is recorded [5]. The sample is identified by comparing the acquired spectrum with well-defined IR absorption tables. An optical absorption based spectrometer consists of a broadband light source, collimating and focusing optics, an optical filter or an interferometer, a sample compartment, and a detector. For ultimate miniaturization, the monolithic integration of all of these components is required, which brings more constraints such as robustness and IC compatibility. Therefore, an optical filter without any moving parts that can be fabricated in an IC-compatible process is the only solution.

Our research group has extensively studied LVOFs in UV, visible and IR wavelength ranges [6-8]. However, a fully functional filter that is suitable for natural gas composition measurement has not been published yet. In this paper, we present two different LVOFs that are designed for short (1.8-2.8 μm) and long (3.0-4.5 μm) wavelength ranges for natural gas analysis. Although the long wavelength range LVOF covers the significant peaks of the main components of natural gas, the short wavelength range LVOF is expected to provide additional information, especially on water content, because of the significant water absorption lines in this part of the spectrum. Moreover, this spectral band is expected to provide additional information of the LVOF-based microspectrometer operation. Both of these optical filters were fabricated in an IC-compatible process using a photoresist reflow technique, followed by transfer etching of the photoresist into the optical resonator layer. The specific advantage of the LVOF-based microspectrometer is that there are no moving parts, while the tapered structure enables the coverage of a broad wavelength with acceptable resolution, as compared to fixed discrete filters with limited wavelength ranges.

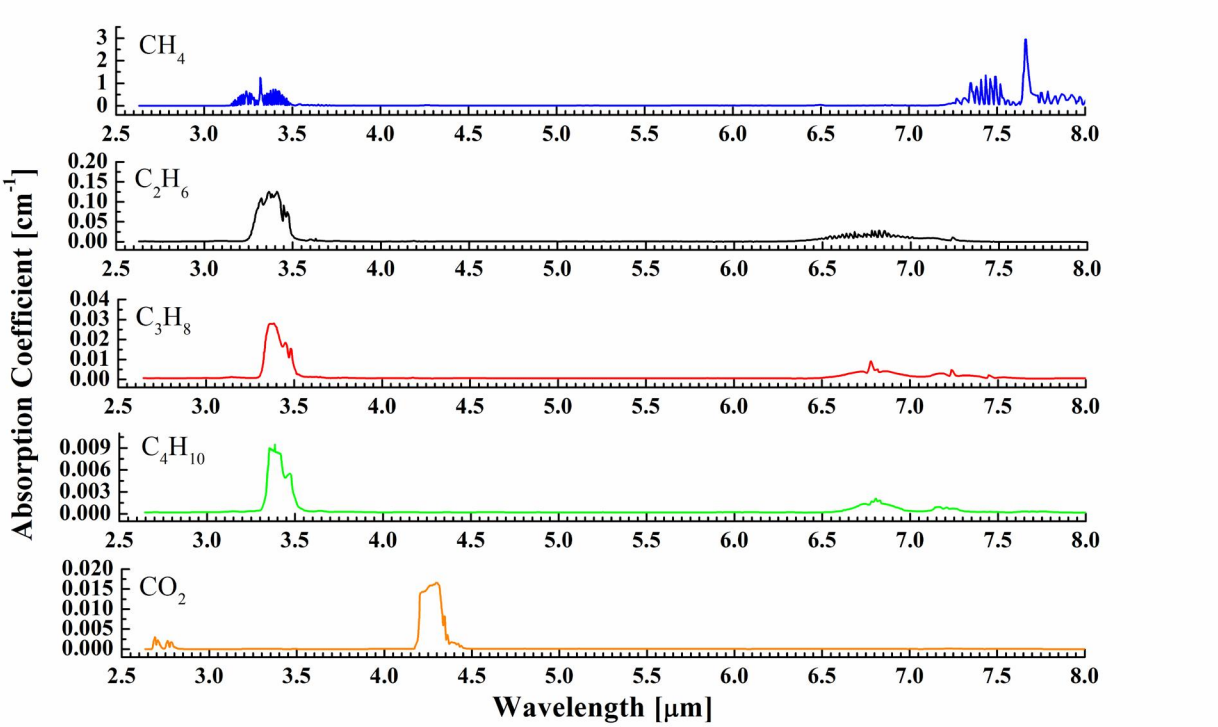

Figure 2: Absorption coefficient of various gases calculated using G-gas concentrations and the NIST database at room temperature for 1 bar total pressure in 2.5-8 μm wavelength range [2].

In the second section of the paper, the optical design of the filters is presented. Then, the fabrication flow is explained in the third section. In the fourth part, the characterization results are shown and the effect of the spot size on resolution is investigated. Finally, the paper is concluded in the fifth section.

2. OPTICAL DESIGN

A Fabry-Perot optical filter is composed of two reflectors with a cavity between, where multiple reflections occur. The thickness of the cavity determines the wavelength to be transmitted through the filter. In an LVOF, the cavity and the top reflector are continuously tapered resulting in a structure with an infinite number of Fabry-Perot optical filters, i.e. LVOF channels, placed next to each other. However, the channel width or the FWHM resolution of the transmission curve at that channel is limited not only by the reflectivity of the mirrors on each side of the cavity but also by the pixel size of the detector that is placed under the filter. Therefore, to achieve high resolution the mirrors must be highly reflective and the pixels should be small.

The reflectors on each side of the cavity in a Fabry-Perot filter are Bragg reflectors that are composed of alternate layers of silicon and silicon-dioxide. The reflectivity of a Bragg reflector increases with both increasing the number of layers and increasing the refractive index contrast between the layer materials. The latter increases the operating bandwidth as well. Therefore, material selection is crucially important in optical filter design to achieve high resolution. Silicon and silicon-dioxide thin-films were selected as high- and low- refractive index materials for LVOF design, respectively since they are IC-compatible materials with good optical contrast that are transparent (i.e. no absorption, zero extinction coefficient) in the desired wavelength range.

The thin-films were deposited using a commercial sputtering machine (FHR MS150, Germany). The sputtering conditions were tuned while the layers were characterized by variable-angle spectro-ellipsometric (VASE) measurements (J.A. Woollam M2000, Lincoln, NE, USA) to optimize the optical properties of the layers. The optical properties of silicon and silicon-dioxide were extracted using Tauc-Lorentz [9] and Cauchy [10] models respectively. However, the ellipsometer data was limited to the spectral range of 250 nm to 1700 nm. To extend the range to the desired wavelength, the Cauchy equation fitted over the ellipsometry data in 1-1.7 μm range was extrapolated up to 5 μm. These values as shown in Figure 3 were then used in the optical thin-film simulations.

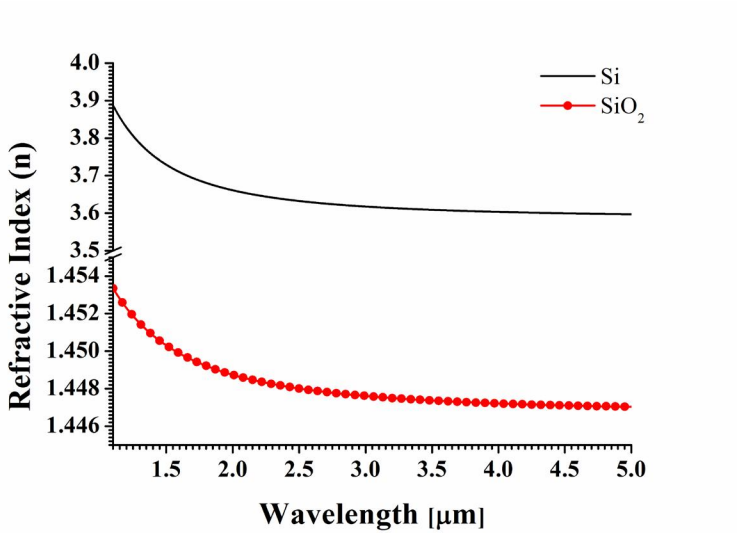

Figure 3: Refractive index of Si and SiO_2.

Two different LVOFs were designed based on these optical constants for operation in the short (1.8-2.8 μm) and the long (3.0-4.5 μm) wavelength ranges. The thickness of the layers used in the design of these LVOFs are listed in Table 2. Both designs employed two Bragg reflectors, one with 4 layers (#1-4) on top of the substrate and another one with 5 layers (#6-10) on top of the cavity. In between these two reflectors, a cavity with linearly varied thickness (#5) is placed. Multi-layer out-of-band blocking filters were placed on top of the LVOFs to block other transmission-orders of the filter.

Table 2: LVOF layers.

Short wavelength	#	Layer	Thickness (nm)
mirror 1	1	SiO_2	345.7
	2	Si	145.3
	3	SiO_2	345.7
	4	Si	145.3
Resonator	**5**	**SiO_2**	**600-1200**
mirror 2	6	Si	145.3
	7	SiO_2	345.7
	8	Si	145.3
	9	SiO_2	345.7
	10	Si	145.3
Out-of-band blocking filter	11	SiO_2	345.7
	12	Si	259.2
	13	SiO_2	622.3
	14	Si	259.2
	15	SiO_2	622.3
	16	Si	259.2
	17	SiO_2	622.3
	18	Si	259.2

Long wavelength	#	Layer	Thickness (nm)
mirror 1	1	SiO_2	553.1
	2	Si	230.4
	3	SiO_2	553.1
	4	Si	230.4
Resonator	**5**	**SiO_2**	**900-1850**
mirror 2	6	Si	230.4
	7	SiO_2	553.1
	8	Si	230.4
	9	SiO_2	553.1
	10	Si	230.4
Out-of-band blocking filter	11	SiO_2	175.5
	12	Si	147.5
	13	SiO_2	350.9
	14	Si	147.5
	15	SiO_2	350.9
	16	Si	147.5
	17	SiO_2	350.9
	18	Si	73.7

Figure 4 shows the expected transmittance of the short wavelength range LVOF simulated using Essential Macleod software (Thin Film Center Inc., Tucson, AZ, USA), with the optical database built on the materials used in this filter and according to the layer thicknesses in Table 2. The cavity thickness is swept from 600 nm to 1200 nm with 50 nm

steps. Although the curves are well-separated, the transmittance is fluctuating. The simulated FWHM resolution varies between 10 and 37 nm.

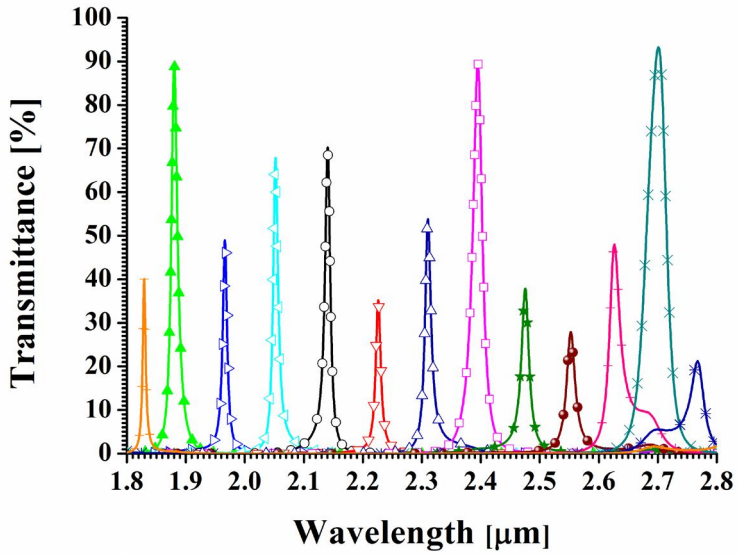

Figure 4: The expected transmittance of the short wavelength range LVOF. As the cavity thickness increases, the transmission curve moves to higher wavelengths.

The simulated transmission curves of the long wavelength range LVOF are given in Figure 5. The cavity thickness is swept from 900 nm to 1850 nm with 50 nm steps. The simulated FWHM resolution is 35 nm and the transmittance is almost constant, 90%, throughout the filter.

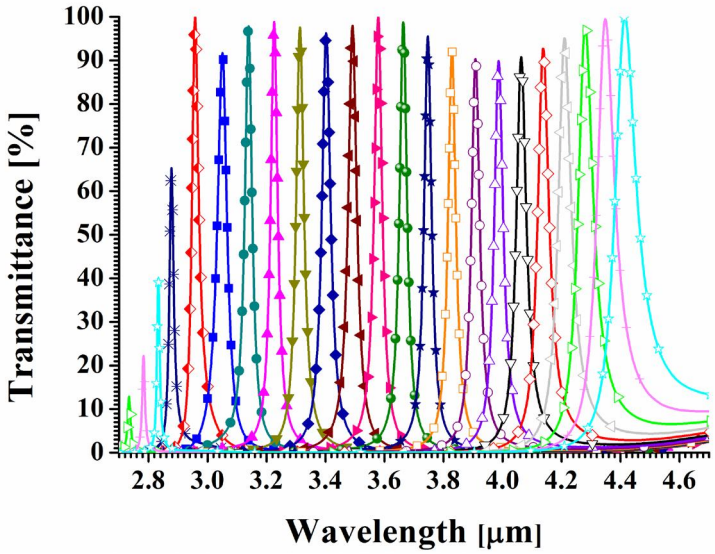

Figure 5: The expected transmittance of the long wavelength range LVOF. As the cavity thickness increases, the transmission curve moves to higher wavelengths.

3. FABRICATION

Fabrication of an LVOF was previously investigated by Emadi *et al.*[11, 12]. In this paper, we applied the same technique of series of trenches with linearly variable spacing, width and/or pitch to create a tapered cavity in the infrared range with different materials.

The process flow is schematically presented in Figure 6. Initially, the bottom dielectric reflector with the layer thicknesses listed in Table 2 and the thick cavity layer with the maximum resonator thickness were sputtered on a silicon wafer. Then, a photoresist layer was spin-coated, patterned, and etched resulting in an array of trenches that are distanced in a linearly variable manner. The following reflow step that includes a chemical-thermal treatment transforms this layer into a smooth tapered resist structure. Later, the tapered photoresist structure was transferred to the underlying cavity layer by plasma etching. Finally, the top reflector and the out-of-band blocking filter were sputtered.

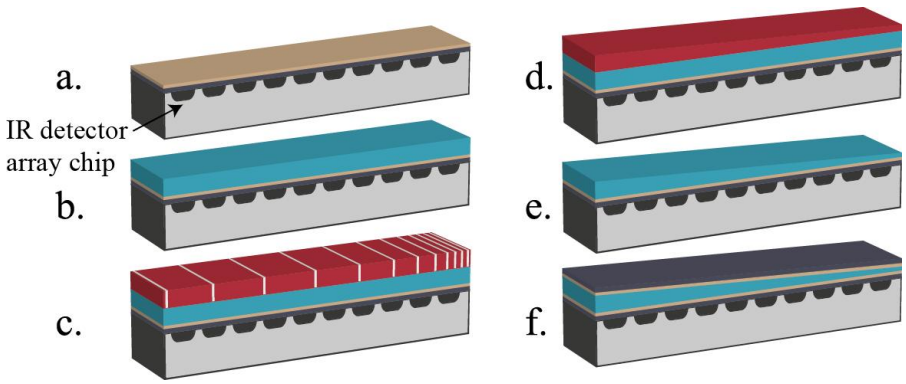

Figure 6: Fabrication process flow: a. depositing the first Bragg reflector, b. depositing the cavity layer, c. patterning, d. reflowing the photoresist, e. transferring the tapered layer into oxide by dry etching, and f. depositing the second multilayer Bragg reflector.

4. CHARACTERIZATION

An LVOF is defined as an infinite number of Fabry-Perot filters placed in a row due to its continuously tapered structure. Therefore to measure the response of an LVOF, the filter is scanned through its length and a spectrum is retrieved at every position. An FTIR spectrometer (Bruker VERTEX70, Germany) employing a mid-IR source and a cooled Mercury Cadmium Telluride (MCT) detector is used for characterization. The LVOF is placed at the sample plane of the instrument and moved along its length by a micrometer stage with 0.5 mm steps for each individual measurement. For each measurement 64 scans are averaged to increase the signal-to-noise ratio (SNR). The smallest available aperture of 0.25 mm size is used to obtain the smallest spot at the sample plane.

The spectral response of the short wavelength range LVOF is shown in Figure 7. Although the transmission peaks follow the simulation results in terms of wavelength, these are mostly widened and the peak transmission is suppressed. Since this wavelength range is dominated by water vapor absorption and it was not possible to purge the sample compartment of the instrument with nitrogen in the current optical setup, the spectrum was highly dominated by water vapor absorption. The double peaks that appear in several measurements are also a result of high frequency oscillations in water vapor absorption spectrum. The FWHM of the transmission peaks varies from 35 nm to 60 nm.

The long wavelength range LVOF on the other hand operates in a range that is free from water vapor absorption lines. Therefore the spectral response is not affected by the ambient, as shown in Figure 8. The measured transmission curves are in accordance with the simulation. The FWHM resolution is approximately 70 nm.

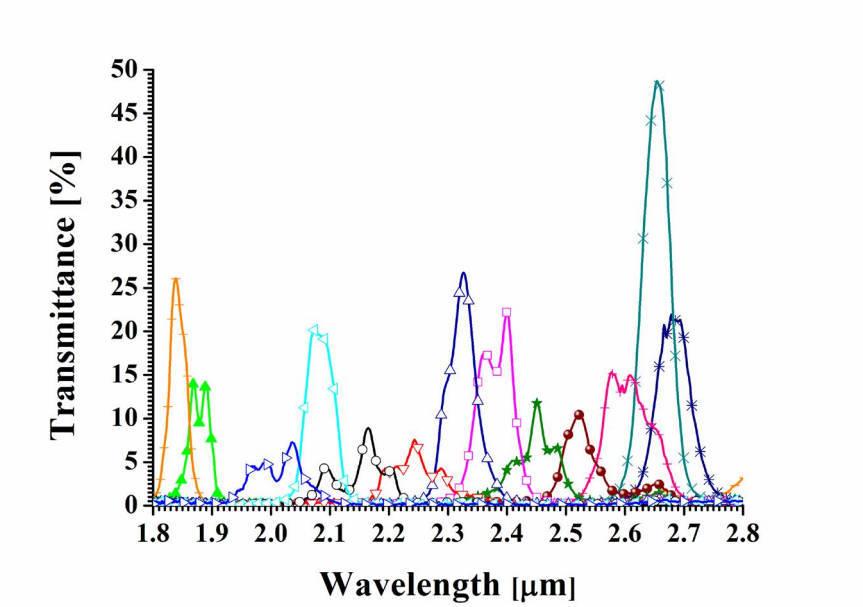

Figure 7: Characterization results of the short wavelength range LVOF.

The number of channels in an LVOF based microspectrometer is determined by the size of the pixels in the detector array that is integrated to the filter. However, a single detector is employed instead of a detector array in the current characterization setup. Therefore, the limitation stems from the size of the spot impinging on the filter, rather than the size of the detector.

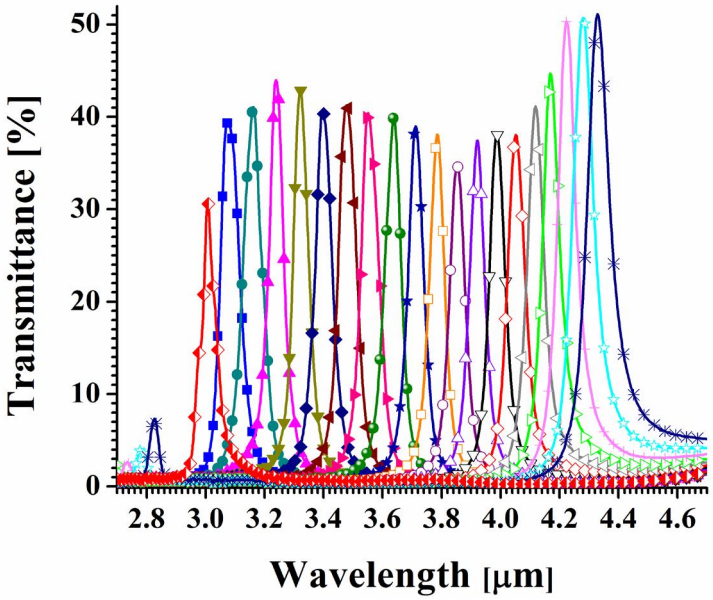

Figure 8: Characterization results of the long wavelength range LVOF.

A simplified model of the characterization setup is designed in Zemax (Radiant Zemax LLC, Redmond, WA, USA) to analyze the effect of the spot size on FWHM. In the FTIR spectrometer, the emission from the source is collected by an elliptical mirror, which then focuses the light on the aperture. Subsequently, the light passes through the aperture and gets collected by a 90° off-axis parabolic mirror with 50 mm diameter and 100 mm effective focal length (EFL). After

propagating from the first parabolic mirror (collimating) to the second (focusing) through the interferometer for 470 mm, the light gets reflected off the focusing mirror. The second 90° off-axis parabolic mirror has a diameter of 50 mm and an EFL of 180 mm. Finally, the beam is focused at the sample plane after passing through a window with 40 mm diameter.

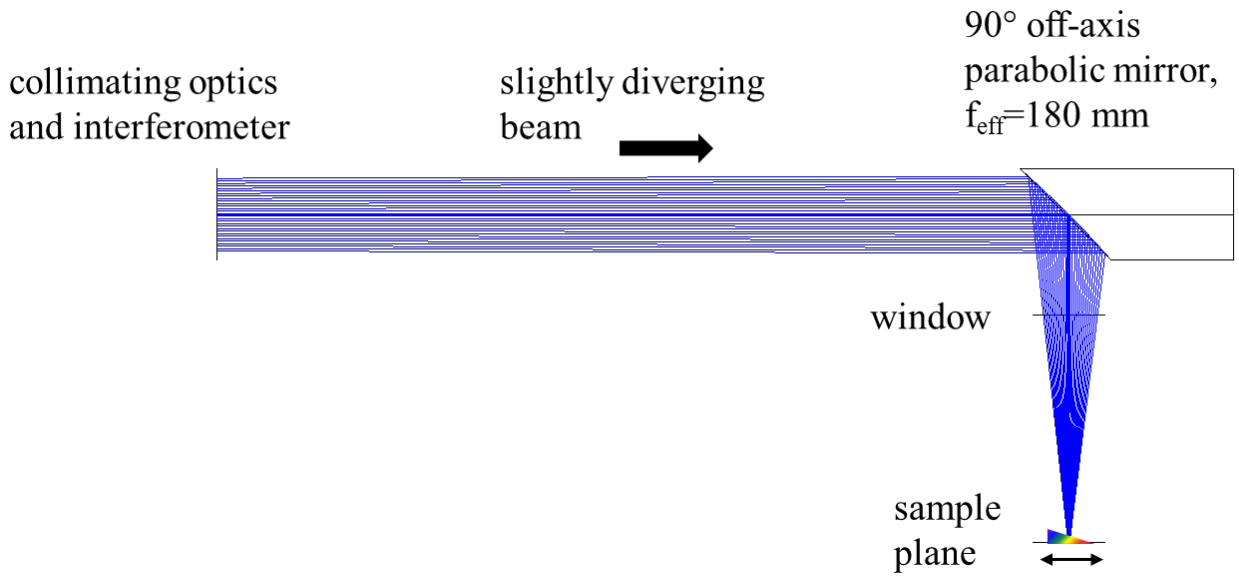

Figure 9: Simplified Zemax layout of the characterization setup.

The Zemax model takes into account the effect of the components before the focusing mirror by introducing a divergence angle to the beam that depends on the aperture size. The Zemax simulation shows that a 0.25 mm sized aperture results in a spot with approximately 0.5 mm geometric radius at the sample plane.

To calculate the effect of the spot size on beam widening, the transmission peak at 3550 nm wavelength is selected in the spectrum of the long wavelength range LVOF. The problem is discretized by dividing the circular spot that impinges on the filter into 11 slits along the length of the LVOF (from -0.5 mm to 0.5 mm with 0.1 mm steps). The power distribution of these slits is extracted from Zemax geometric image analysis as shown in Figure 10.

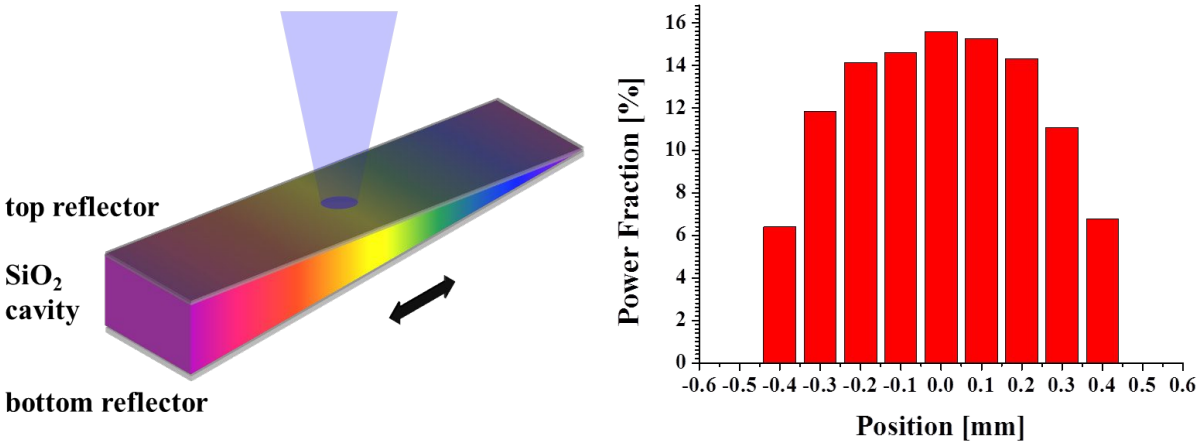

Figure 10: The sketch of LVOF with the light spot impinging on it (left), and power distribution of the light spot (right).

The long wavelength range LVOF has a taper angle of 0.005°. This results in a 9 nm cavity thickness change for every 0.1 mm movement along the length of the filter. Therefore, 11 consecutive transmission curves are simulated in the optical thin film design tool that correspond to the slits in the spot. The simulation results are shown in Figure 11 for

cavity thicknesses varying between 1238 nm and 1328 nm with 9 nm steps, while keeping the center peak at the selected wavelength of 3550 nm.

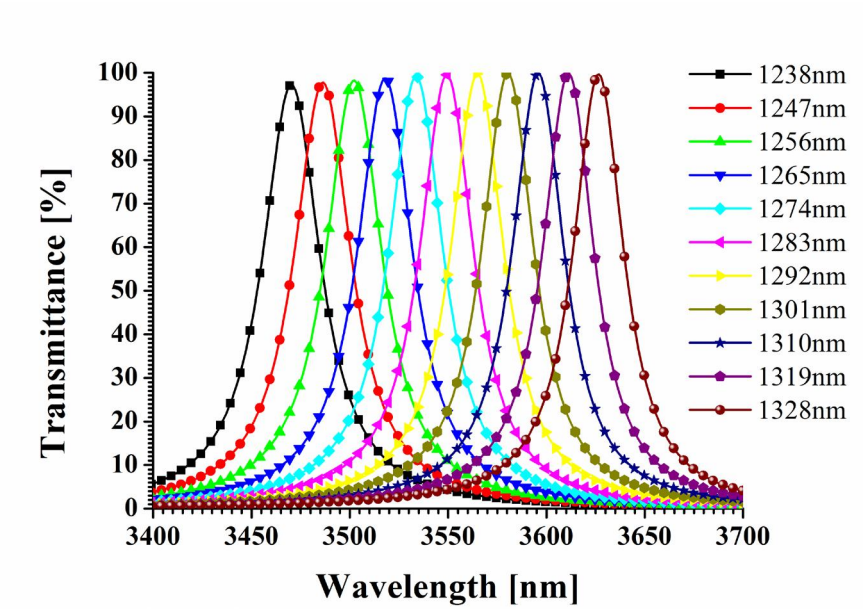

Figure 11: Simulated transmission curves with thicknesses varying from 1238 nm to 1328 nm with 9 nm steps.

The power-weighted sum of these transmission curves resulted in a widened curve with 124 nm calculated FWHM while the designed and the measured FWHM resolutions are 33 nm and 70 nm respectively (Figure 12). The measured and the calculated transmittance levels (40%) on the other hand fit almost perfectly.

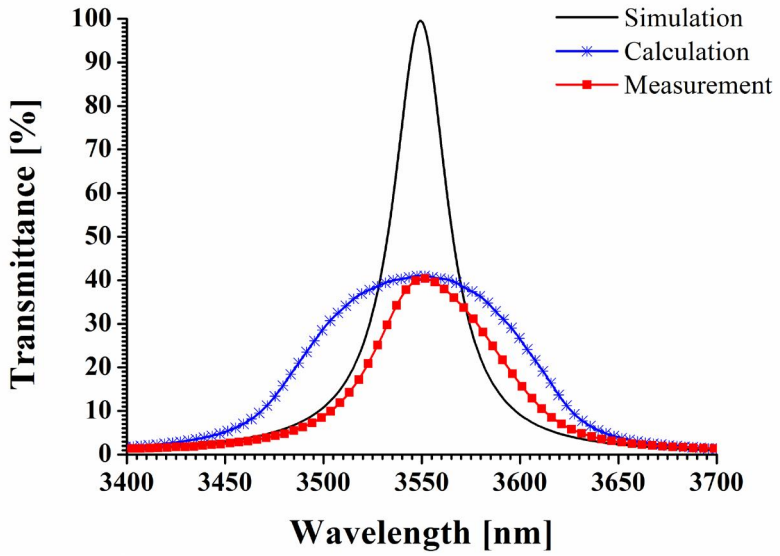

Figure 12: Optical thin film simulation, power distribution calculation and actual measurement results for the transmission curve that has a peak at 3550 nm.

5. CONCLUSION

In this paper, we have presented the design, fabrication, and characterization of two LVOFs to be used for natural gas composition measurement. The short and the long wavelength range LVOFs have a measured FWHM of 35-60 nm and

70 nm respectively. The performance of the short wavelength range LVOF was deteriorated by strong water vapor absorption in that spectral region. We have also shown the effect of beam size on filter resolution. The optical thin film simulation, the power distribution calculation, and the actual measurement results were presented for the transmission curve centered at 3550 nm. In addition to the transmission curve widening, the effect of the beam size on transmittance was also provided in the article.

Consequently, we proved that these two filters combined together exhibit sufficient performance for natural gas analysis. The resolution can be further improved by post processing algorithms. Authors are currently working on integrating the filters with the rest of the components of the spectrometer.

ACKNOWLEDGEMENTS

This work has been supported by the Dutch technology foundation STW under grant DEL.11476. The devices were fabricated at MC2 of Chalmers University, Sweden. The authors would like to thank Herman Schreuders for helping with the measurements.

REFERENCES

[1] "Report on Gas Composition," Directoraat-generaal voor Energie, Telecom en Markten 2011.
[2] NIST Mass Spec Data Center and S. E. Stein, director, "Infrared Spectra," in *NIST Chemistry WebBook, NIST Standard Reference Database Number 69*, P. J. Linstrom and W. G. Mallard, Eds., ed Gaithersburg MD, 20899: National Institute of Standards and Technology.
[3] *NL Oil and Gas Platform*. Available: http://www.nlog.nl/
[4] J. Hodgkinson and R. P. Tatam, "Optical gas sensing: a review," *Measurement Science and Technology,* vol. 24, p. 012004, 2013.
[5] N. V. Tkachenko, *Optical Spectroscopy: Methods and Instrumentations*: Elsevier Science, 2006.
[6] A. Emadi, H. Wu, G. de Graaf, P. Enoksson, J. H. Correia, and R. Wolffenbuttel, "Design, fabrication and measurements with a UV linear-variable optical filter microspectrometer," 2012, pp. 84390V-84390V-10.
[7] A. Emadi, H. Wu, G. de Graaf, and R. Wolffenbuttel, "Design and implementation of IR microspectrometers based on linear-variable optical filters," pp. 84391O-84391O, 2012.
[8] A. Emadi, H. Wu, G. de Graaf, and R. Wolffenbuttel, "Design and implementation of a sub-nm resolution microspectrometer based on a Linear-Variable Optical Filter," *Opt. Express,* vol. 20, pp. 489-507, 2012.
[9] G. E. Jellison and F. A. Modine, "Parameterization of the optical functions of amorphous materials in the interband region," *Applied Physics Letters,* vol. 69, pp. 371-373, 1996.
[10] H. G. Tompkins and W. A. McGahan, *Spectroscopic Ellipsometry and Reflectometry: A User's Guide*: Wiley, 1999.
[11] A. Emadi, H. Wu, S. Grabarnik, G. De Graaf, K. Hedsten, P. Enoksson, J. H. Correia, and R. F. Wolffenbuttel, "Fabrication and characterization of IC-Compatible Linear Variable Optical Filters with application in a micro-spectrometer," *Sensors and Actuators A: Physical,* vol. 162, pp. 400-405, 2010.
[12] A. Emadi, H. Wu, S. Grabarnik, G. De Graaf, and R. Wolffenbuttel, "Vertically tapered layers for optical applications fabricated using resist reflow," *Journal of Micromechanics and Microengineering,* vol. 19, p. 074014, 2009.